Carbohydrate Polymers 254 (2021) 117462

Contents lists available at ScienceDirect

Carbohydrate Polymers

journal homepage: www.elsevier.com/locate/carbpol

# Structural and immunological studies on the polysaccharide from spores of a medicinal entomogenous fungus *Paecilomyces cicadae*

Yin Chen [a,*], Teng Wang [a], Xing Zhang [b], Fuming Zhang [c], Robert J. Linhardt [c,*]

[a] College of Food and Pharmacy, Zhejiang Ocean University, Zhoushan, Zhejiang 316000, China
[b] School of Food Science and Pharmaceutical Engineering, Nanjing Normal University, Nanjing, Jiangsu 210023, China
[c] Departments of Chemistry and Chemical Biology, Biology, Chemical and Biological Engineering, and Biomedical Engineering, Center for Biotechnology and Interdisciplinary Studies, Rensselaer Polytechnic Institute, Troy, NY 12180, USA

ARTICLE INFO

*Keywords:*
Fungus polysaccharide
Structure
Immunostimulating activity
Macrophages
Cell membrane receptor

ABSTRACT

A neutral branched heteropolysaccharide (Pc0−1) was purified from the spores of *Paecilomyces cicadae*, which parasitized in the bamboo cicada (*Platylomia pieli* Kato). The structure of Pc0−1 was analyzed by HPLC, IR, methylation and NMR spectroscopy. The results reveal that Pc0−1, with an average molecular weight of 18 × $10^3$ kDa, consists of glucose, galactose, mannose and arabinose in the molar ratio of 8:5:4:1. Some of the glucose residues have methyl modification at *O*-6 position. The Pc0−1 polysaccharide has a core structure containing 1,2-linked α-D-Man*p* residues as the backbone and branches at the *O*-3 and *O*-6 of the α-D-Man*p* residues. The inner part of the side-chains is comprised of 1,4-linked α-D-Glc*p* and 1,4-linked 6-*O*-Me-α-D-Glc*p* residues. 1,2-linked β-Gal*f* and minor 1,4-linked Ara*p* and 1,3 or 4-linked Ara*p* residues were occasionally linked at the outside of the side-chains. The side-chains have a single terminal residue of α-D-Glc*p*, α-Man*p*, β-Gal*f* or minor Ara*p* (minor). Studies on the bioactivity of Pc0−1 on the macrophages show it exhibit moderate immunostimulating activity through increasing the production of nitric oxide (NO) and enhancing the secretion of major inflammatory cytokines by macrophages, such as TNF-α, IL-1β, IL-6, in RAW 264.7 cells. We examined the effect of Pc0−1 on induced NO and cytokine production in macrophages using anti-PRR antibodies to investigate the membrane receptor for the polysaccharide. The results show that Pc0−1 mainly activates macrophages through their mannose receptor (MR). TLR4 and TLR2 also participated in the recognition of Pc0−1.

## 1. Introduction

*Cordyceps sinensis* (Berk.) Sacc is an entomogenous fungus that selectively infects bat moth (*Hepialus armoricanus*) larvae of the genus *Cordyceps* (*Clavicipitaceae*), know as DongChongXiaCao (winter worm-summer grass) in Chinese, or Tochukaso in Japanese. In late summer or early autumn, the larvae of bat moth are infected by *Cordyceps sinensis* and are gradually consumed by the fungal mycelia. In winter, the larvae become "stiff worms'' and in spring and early summer of the following year, a fruiting body forms on the larvae head, which then grows and emerges from the ground like a grass (Yan et al., 2014). Dong Chong Xia Cao, as a valuable tonic in traditional Chinese medicine, is a made from the combination of the fruiting body of *C. sinensis* and the host insect (Nie et al., 2018). The numberous pharmacological effects of this medicinal fungus can be attributed to its chemical components, including polysaccharides, proteins, nucleotides, mannitol, ergo sterols, aminophenols, fatty acids, and trace elements (Prasain, 2013). Several reviews on the properties of the compounds and their bioactivities of *C. sinensis* have been published in recent years (Yan et al., 2014). Polysaccharides in particular represent one of the most abundant and bioactive constituents that have been extracted from the fruiting bodies, cultured mycelium and fermentation broth (Huang et al., 2018; Wang et al., 2018). Nutraceutical and health supplement products have been developed using polysaccharides from *C. sinensis*. Similar to *C. sinensis*, *Paecilomyces tenuipes* (Peck) Samson are also entomogenous fungi, which are the anamorphic stage of *Cordyceps* (Takano et al., 2005). These fungi, and the host insects have been used as traditional natural health foods beneficial in Japan, Korea and China due to their biological activities including immunomodulatory activity, anti-aging, antitumor activity, anti-inflammation effects and amelioration of renal function (Olatunji et al., 2016; Wang et al., 2019; Xu et al., 2018). *P. cicadae* and *C. sinensis* have similar properties and functions (Nxumalo et al., 2020);

* Corresponding authors.
*E-mail addresses:* mojojo1984@163.com (Y. Chen), linhar@rpi.edu (R.J. Linhardt).

https://doi.org/10.1016/j.carbpol.2020.117462
Received 23 June 2020; Received in revised form 25 November 2020; Accepted 25 November 2020
Available online 1 December 2020

however, few studies have been reported on the structure and bioactivity of polysaccharides from *P. cicadae*.

Fungal spores, containing full genetic materials and biological substances, have greater pharmaceutical values than the fruit bodies, particularly *Ganoderma* spores (Bao et al., 2001). Structural analysis and biological properties of bioactive glucans from *G. lucidum* spores have been investigated (Wang et al., 2017). In this study, the structure of the polysaccharide from the spores of *P. cicadae* was analyzed, and its immunoregulatory activity was evaluated. This study provides useful information on the characteristics of polysaccharide from the *P. cicadae* spores, and will benefit further investigations into the utilization of similar medicinal fungi.

## 2. Materials and methods

### 2.1. Materials and reagents

*P. cicadae* parasitizing in the bamboo cicada (*Platylomia pieli* Kato) was collected from the bamboo forest in the Zhoushan archipelago, China. An assay kit for nitric oxide (NO) was purchased from Beyotime Biotechnology Co. (Shanghai, China). Assay kits for interleukin-6 (IL-6) and tumor necrosis factor-alpha (TNF-α) were purchased from Multi Sciences Biotechnology Co. (Hangzhou, China). Anti-mannose receptor antibody (anti-MR), anti-toll-like 2 antibody (anti-TLR2) and anti-toll-like 4 receptor antibody (anti-TLR4) were obtained from Abcam, Inc. (Cambridge, MA, USA). Other reagents were of analytical grade and purchased from Aladdin industrial Co. (Shanghai, China).

### 2.2. Extraction and purification of polysaccharides

The spores of *P. cicadae* were dried at 50 °C for 48 h and defatted with petroleum ether (1:10, w/v) in the Soxhiet extractor for 12 h. Enzyme assisted extraction method was used to extract the polysaccharide. In brief, 25 *g* of the defatted spores, 500 mL distilled water and neutral proteinase from *Bacillus polymyxa* (activity 50 units/mg) (0.8 %, w/ v) were stirred at 45 °C for 2 h. The enzymatic digestion was terminated by boiling for 30 min. The solution was filtered, and then concentrated to 1/4 of the original volume, followed by precipitation with 4 vol of ethanol at 4 °C for 48 h The precipitate was collected by centrifugation (1760 *g*, 15 min). The crude polysaccharide product was dialyzed and lyophilized (Zhou et al., 2019).

The crude polysaccharides were purified by anion-exchange chromatography using a Q Sepharose Fast Flow column (300 × 30 mm), eluted with a step-wise gradient of 0, 0.1, 0.25 and 0.5 M NaCl for 2 column volume. The fractions containing sugar and eluted with water were gathered, dialyzed, freeze–dried and further purified by gel permeation chromatography using a Superdex 75 column (70 × 2 cm) eluted with 0.2 M $NH_4HCO_3$ at a flow rate of 0.3 mL/min. The major polysaccharide fractions were pooled, freeze–dried and named as Pc0−1.

### 2.3. Physicochemical properties analysis

Purity and molecular weight distribution were determined by high performance gel permeation chromatography (HPGPC) on a TSK gel G3000$PW_{XL}$ column (7.8 mm × 30.0 cm, Tosoh, Japan) at 35 ℃ with refractive index detection (Agilent 1100 Series) with 0.2 mol/L $Na_2SO_4$ as the mobile phase at a flow rate of 0.5 mL/min. 20 μL of 1% sample solutions in 0.2 mol/L $Na_2SO_4$ was injected. The molecular weight was estimated by reference to a calibration curve made by a set of dextran T-series standards (*Mw*: 708, 344, 200, 107, 47.1, 21.1 and 9.6 kDa). The Mw and the polydispersity which is the ratio of Molecular weight in weight/Molecular weight in number were calculated by the GPCW32 Chromatographic workstation.

Protein content was measured by the method of Bradford. Total carbohydrate content was determined by the phenol-sulfuric acid assay using glucose as the standard. After complete acid hydrolysis with 2 M TFA(trifluoroacetic acid) at 5 mg/mL and 105 ℃ for 6 h, the monosaccharide compositions were determined by HPLC (Agilent 1260) after 1-phenyl-3-methyl-5-pyrazolone (PMP) pre-column derivatization. Standard sugars (L-arabinose, L-rhamnose, L-fucose, D-galactose, D-galacturonic acid, D-glucose, D-glucuronic acid, D-glucosamine, D-mannose, D-xylose, and) at different concentrations (10−100 μg/μL) were loaded in HPLC to obtain the standard curves of peak area *vs*. concentration. The molar ratios of the monosaccharides were calculated on the basis of the peak areas and the standard curves.

Sugars in the hydrolysates were converted into their alditol acetates by reduction with $NaBH_4$ and analyzed by GC–MS using a DB-5 ms column to identify the unknown monosaccharide in Pc0−1 (Wang et al., 2019; Yang et al., 2007). The method in detail was as the method *2.5*.

### 2.4. IR spectroscopy

The polysaccharide was mixed with KBr powder, ground and then pressed into a 1 mm pellets for FTIR measurement in the frequency range of 4000–500 $cm^{-1}$. FTIR spectrum of the polysaccharide was measured on a Nicolet Nexus 470 spectrometer (Thermo Scientific, Waltham, MA, USA).

### 2.5. Partial acid hydrolysis and methylation analysis

Partial acid hydrolysis of Pc0−1 was performed using previously described methods (Ishurd & Kennedy, 2005; H. Wang et al., 2015). Briefly, the polysaccharide (10 mg) was depolymerized with 0.01 M trifluoroacetic acid at 105 °C for 2 h. The hydrolyzate was evaporated to dryness and dissolved in 50 % ethanol. The soluble and insoluble products were recovered by centrifugation (3600 × *g*, 10 min), vacuum-dried and designated as Pc0−1S1 and Pc0−1P1, respectively. Next, Pc0−1P1 was further depolymerized using 0.1 M trifluoroacetic acid at 105 °C for 2 h and treated with the same procedures as previously described. The soluble and insoluble products in 50 % ethanol were named as Pc0−1S2 and Pc0−1P2, respectively. Pc0−1S1, Pc0−1S2 and Pc0−1P2 were subjected to monosaccharide compositional analysis.

In addition to the monosaccharide composition, the glycosidic linkages in Pc0−1 and the hydrolysate (P-2) were further investigated by GC–MS using methylation analysis. The methylation analysis of Pc0−1and Pc0−1P2 was performed according to a modified Hakomori method using sodium hydride in dimethyl sulfoxide and methyl iodide. The methylated sample was hydrolyzed as described above, reduced with sodium borodeuteride and converted into partially methylated alditol acetates and analyzed by GC–MS on a HP6890II/5973 instrument using a DB-5 ms fused silica capillary column (0.25 mm × 30 m) (Agilent Technologies Co., Ltd., USA). The temperature was increased from 100 °C to 220 °C at a rate of 5 °C /min then maintained at 220 °C for 5 min with helium as carrier gas. The peaks on the chromatogram were identified from their retention times and the mass fragmentation patterns (Zhou et al., 2019).

### 2.6. NMR spectroscopy

Freeze-dried Pc0−1(80 mg) were dissolved in 400 μL of $D_2O$ (99.96 atom %) and lyophilized twice to exchange exchangeable protons and transferred to a 5-mm NMR tube. $^1H$ NMR, HSQC NMR, $^1H$-$^1H$ COSY and TOCSY were performed on a Bruker 800-MHz NMR spectrometer and acquisition of the spectra was carried out using Topspin 2.1.6 software. All spectra were acquired at a temperature of 298 K.

### 2.7. Determination of macrophage activation

#### 2.7.1. Cell viability assay

The impact of different concentrations of Pc0−1 (50−400 μg/mL) on the viability of RAW264.7 cells was analyzed using the 3-(4, 5-

dimethylthiazol-2-yl)-2, 5-diphenyltetrazolium bromide (MTT) assay. RAW264.7 cells were purchased from the Type Culture Collection of Chinese Academy of Sciences (Shanghai, China). The cells were pre-incubated in 96-well plate at density of $1 \times 10^6$ cells/mL per well for 24 h and then were respectively cultured with LPS (2 μg/mL) and different concentrations of Pc0−1 for 24 h. After incubation, the cells were stained with MTT (30 μL/well) to a final concentration of 0.5 mg/mL for 4 h at 37 °C in dark, and then the supernatants were removed before adding DMSO (100 μL/well). Finally, the absorbance was measured at 570 nm by microplate ELISA reader (Wu et al., 2017).

#### 2.7.2. Measurement of ROS generation

ROS production by RAW264.7 was measured using the fluorescent probe DCFH-DA (2,7-dichlorodihydrofluorescein dilacerate) (Sun et al., 2005). Briefly, the RAW264.7 cells were seeded at $5 \times 10^5$ cells/well in glass bottom cell culture dishes overnight. LPS (2 μg/mL), and the various concentrations of polysaccharides (50−400 μg/mL) were added into each well, and incubated for 24 h at 37 °C. Then, all the culture medium were removed before adding DCFH-DA (10 μL/well) for 30 min at 37 °C. Finally, the cells were washed twice with PBS. The degree of fluorescence was detected at 485 nm excitation and at 535 nm emission using fluorescence microscopy.

#### 2.7.3. Determination of phagocytic uptake

The phagocytic uptake activity of the macrophages was determined using the fluorescent-red latex beads (2 μm) and neutral red. RAW264.7 cells were seeded at $1 \times 10^4$ cells well $^{-1}$ in a 96-well plate and incubated at 37 °C for 24 h. Then, DMEM medium, LPS (2 μg/mL) or the various concentrations of polysaccharides (50−400 μg/mL) were added into each well, and incubated for 24 h at 37 °C. Each concentration was repeated in three wells. Culture media were removed and 0.1 % latex beads (red fluorescent, excitation/emission of 553/635 nm) or 0.075 % neutral red was added, and incubated for 30 min. The cells were washed twice with phosphate-buffered saline (PBS). For analysis of cell phagocytic uptake of fluorescent red-aqueous suspension, the cells were stained with MitoTracker (mitochondrial, green, excitation/emission of 490/516 nm) for 15 min. The phagocytic activity of RAW264.7 cells was determined using laser-scanning confocal microscopy (FV 1000, Olympus Co., Tokyo, Japan) after staining with MitoTracker. For analysis of cells phagocytic uptake of the neutral red, cell lysing solution (150 μL/well) were added into each well and cells were cultured for 1 h at 37 °C. The absorbance was evaluated in an ELISA reader at 570 nm. Pinocytic ability (%) $= \frac{A_{sample}}{A_{control}} - 1 \times 100\%$, where $A_{control}$ was the absorbance of control without the tested samples, and $A_{sample}$ is the absorbance in the presence of the tested samples (Kim et al., 2012).

#### 2.7.4. Measurement of inducible nitric oxide synthase (iNOS) production

The RAW264.7 cells were pre-incubated in 96-well plate at density of $1 \times 10^6$ cells/mL per well for 24 h. Then, LPS (2 μg/mL) as the positive control and the various concentrations of polysaccharides were added into each well, and these cells were incubated for 24 h at 37 °C. cell culture supernatants were collected by centrifugation at 110 *g* for 8 min at 4 °C and stored at −20 °C, and the iNOS level was determined by ELISA kit (Shanghai mlbio Biotechnology Co. Ltd., Shanghai, China), according to the manufacturer's instructions.

#### 2.7.5. Cytokine assays

The RAW264.7 cells were pre-incubated in 96-well plate at density of $5 \times 10^5$ cells/mL per well for 24 h with LPS (2 μg/mL) with various concentrations of polysaccharides as above. The production of IL-1β, IL-6, IL-12 and TNF-α in the cell culture supernatants were analyzed using an ELISA kit (Shanghai mlbio Biotechnology Co. Ltd.), according to the manufacturer's instructions (Xu et al., 2012).

#### 2.7.6. Inhibition of cytokine production using anti-PRR antibodies

The RAW264.7 cells were pre-incubated in 96-well plate at density of $1 \times 10^6$ cells/mL per well for 24 h. After the culture media removed, 100 μL anti-MR anti-TLR2 and anti-TLR4 (5 μg/mL) were added to each well 1 h prior to treatment with 200 μL polysaccharides (200 μg/mL) for 24 h at 37 °C. After incubation, the productions of cytokine in the cell culture supernatants were analyzed by cytokine assay (Wu et al., 2018).

#### 2.7.7. Statistical analysis

All data obtained in this study were processed statistically and divergences were presented as mean ± SD. SPSS 16.0 for Windows (Pearson Co., Beijing, China) was used and $P < 0.05$ indicated significance differences.

## 3. Results and discussion

### 3.1. Extraction and purification of polysaccharides

Enzyme assisted extraction of the defatted spores was used to destroy the cytoderm and promote the dissolution of polysaccharides, resulting in a high extraction yield of 5.6 %. The crude polysaccharides were separated to three fractions (Distilled water, 0.1 M NaCl and 0.25 M NaCl eluted fractions) on the anion-exchange chromatography and named as Pc0, Pc0.1 and Pc0.25, respectively. Pc0 (60 % yield of the crude polysaccharide) and Pc0.1 (25 % yield of the crude polysaccharide) were collected according to the chromatography profile (Fig. 1a). Pc0 was further purified on a Superdex 75 column, and a purified neutral polysaccharide Pc0−1 (75 % of Pc0) was obtained.

### 3.2. Purity, chemical and composition analysis of polysaccharides

The HPGPC analysis results showed the Pc0−1 had a single symmetrical peak in Fig. 1c. The relative Mw of Pc0−1 was calculated to be $18 \times 10^3$ kDa, which was similar to the values of the many reported similar fungal polysaccharides. A fucoglucogalactan from the fruiting bodies of the fungus *Hericium erinaceus* had the molecular weight of $19 \times 10^3$ kDa (Zhang et al., 2007). A 3-*O*-methyl-D-galactose-containing neutral polysaccharide from the fruiting bodies of *Phellinus igniarius* had the molecular weight of $17 \times 10^3$ kDa (Yang et al., 2007). The polydispersity of Pc0−1 was 1.24, a relative narrow distribution, which further suggested its homogeneity. Pc0−1 did not contain protein by the Bradford method. Total carbohydrate content was determined to be 93.8 %. The monosaccharide composition analysis showed that Pc0−1 was composed of Man, Glc, Gal and Ara at the molar ratio of 4:8:5:1, indicating that it was a neutral heteropolysaccharide. In addition, another peak was observed from the HPLC between Man and GlcN that did not match any of our monosaccharide standards. Because of no acidic or basic sugar existed in Pc0−1, the hydrolysates of Pc0−1 were reduced by $NaBH_4$ and converted into alditol acetates by acetic anhydride. Combined with the monosaccharide composition in HPLC, the unknown sugar could be 6-*O*-methyl glucose which was determined by the additional signal of 1,2,3,4,5-$Ac_5$-6-Me-D-glucitol (*m/z*, 8,799,129,139,157, 185,201,231 and 259) from the GC–MS. The total ion current chromatogram and MS of partially *O*-methylated alditol acetates of Pc0−1 are shown in the supplementary material.

*P. cicadae* is a valuable Chinese caterpillar fungus that has been extensively used as a tonic food and medicine for centuries. Different polysaccharides were isolated from *P. cicadae* obtained from different sources. Two heteropolysaccharides from *Isaria cicadae* Miquel (Guangdong Province, China) were composed of Man, Glc and Gal at the ratio of 1.37:1.70:1.00 and 1.04:5.41: 1.00 (Xu et al., 2018). A water-soluble galactomannan, isolated from the rod-like ascocarps of *Cordyceps cirudae,* was composed of Man and Gal in the molar ratio of 4:3 (Ukai et al., 1982). Two polysaccharide components, isolated from *Cordyceps cirudae* (Jiangsu Province, China), had glucose as the main monosaccharide (47.7 % and 79.7 %, respectively) and a small amount

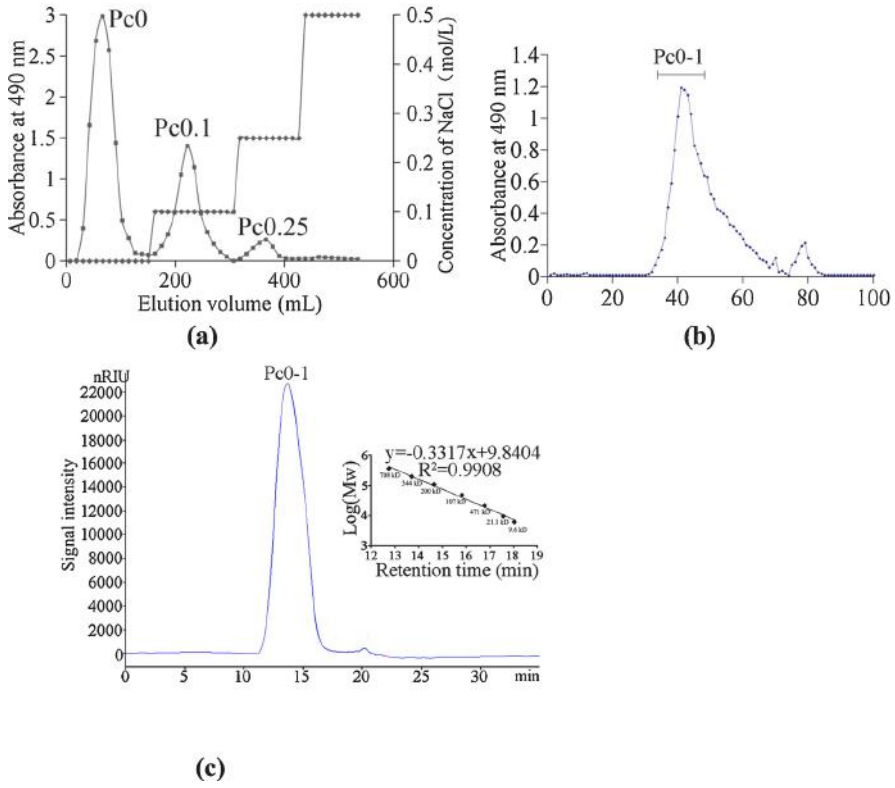


**Fig. 1.** Purification and HPGPC chromatogram of the polysaccharides from the spore of the medicinal fungus *Paecilomyces cicadae*. (a) Three fractions Pc0, Pc0.1 and Pc0.25 were isolated on Q Sepharose Fast Flow column; (b) Purification of Pc0 on a Superdex75 column; (c) HPGPC chromatograms of Pc0-1 on TSKgel G3000PWXL column and standard curve of molecular weights.

of Man and Gal (Olatunji et al., 2016). A heteropolysaccharide from cultured mycelium of *Paecilomyces cicadae* was primarily composed of Glc, Gal and Man in a molar ratio of 23.8:2.1:1.0 (Wang et al., 2019). From these results, we can understand that *P. cicadae* can produce various polysaccharides. Although the monosaccharide compositions change with different resources, growth conditions and insect hosts, all the polysaccharides have similar characteristics as neutral sugars. Man, Glc and Gal are very common monosaccharides in *P. cicadae* polysaccharides and Glc is the major sugar for most polysaccharides. Some polysaccharides contain methylated sugar. For Pc0−1, isolated from bamboo cicada infected *P. cicadae*, it shows a similar structure pattern as other polysaccharides from *P. cicadae*, except it has a small amount of Ara.

### 3.2.1. IR spectrum of the polysaccharide

Infrared presented the overall structural feature of polysaccharides and could be used as the fingerprint of polysaccharide. Infrared spectrum of Pc0−1 was used to analyze the glycosidic bond configuration and reveal major functional groups. The IR spectrum of Pc0−1 is shown in Fig. 2. A prominent band near 3359 $cm^{-1}$ corresponded to the stretching vibration of OH. The signal at 2933 $cm^{-1}$ was due to CH— stretching. The characteristic band at 1058 $cm^{-1}$ belongs to the asymmetrical stretching vibration of C—OC— glycosidic bonds, which is a characteristic band of sugar ring. The absorbance at 1650 $cm^{-1}$ indicates bound water and the absorption peak at 1414 $cm^{-1}$ is attributed to characteristics of $CH_2$ deformation mode. The presence of a typical band in the IR spectrum of Pc0−1 at 870 $cm^{-1}$ was assigned to the characteristic configurations of β glycosides. In addition, the peaks at 808 $cm^{-1}$ confirmed the characteristic absorption of mannose (Zhou et al., 2019).

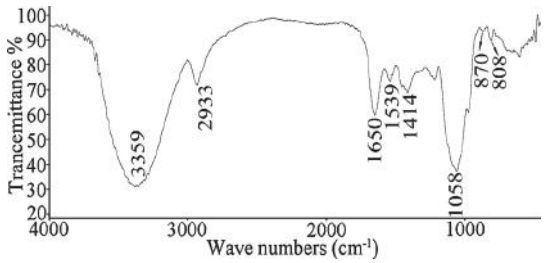


**Fig. 2.** IR spectrum of Pc0-1.

### 3.3. Partial acid hydrolysis and methylation analysis

Pc0−1 was composed of Glc, Man, Gal, Ara and 6-*O*-methyl glucose. Due to the structural complexity, a controlled partial acid hydrolysis with mild acid was employed to characterize the distribution of the monosaccharides in Pc0−1. In general, the hydrolysis of branches is relatively easier than the hydrolysis of the backbone of a polysaccharide. In the hydrolysis process, an increased duration of hydrolysis, results in the effective step-by-step removal of the side-chains without significantly influencing the structure of the backbone (Qiu et al., 2020).

Three sub-fractions (S-1, S-2 and P-2) were obtained under partial acid hydrolysis. The monosaccharide components of these are shown in Table 1. Ara only existed in S-1. The evidence that S-1 is mainly composed of Gal and Ara indicates that Gal and Ara are present in the side-chains and are sensitive to acid hydrolysis. On increasing the acid concentration (from 0.01 M to 0.1 M TFA), the content of Gal in S-2 is reduced. In S-2, the amounts of Glc and Man are much greater than Gal.

**Table 1**
Monosaccharide composition of Pc0-1 and the products after partial acid hydrolysis.

| Sample | Monosaccharide composition (% mol) | | | |
|---|---|---|---|---|
| | Man | Glc | Gal | Ara |
| Pc0−1 | 22.2 | 44.4 | 27.8 | 5.6 |
| S-1 | 5.4 | 7.2 | 69.3 | 18.1 |
| S-2 | 30.0 | 51.6 | 18.4 | — |
| P-2 | 82.9 | 12.0 | 5.1 | — |

Fraction P-2 is primarily composed of Man suggesting that Man comprised the core structure of Pc0−1 and that Glc was in the side-chain. The results of gradual acid hydrolysis showed that the backbone of Pc0−1 was primarily composed of Man, while the side-chain was composed of Glc, Gal and Ara. Gal and Ara were mainly located on the terminal region of the side-chain and easily hydrolyzed (Chen et al., 2016).

The results of methylation analysis demonstrated that the complex structure of Pc0−1 was due to a diverse linkage pattern (Table 2). The mol% of each derivative was calculated by dividing the peak area from the total ion chromatograms by the molecular weight of the PMAA (Sims et al., 2018) Ara residues had terminal Ara*p*, 1,4-Ara*p* and 134-Ara*p* linkages; Gal residues had terminal Gal*f* and 1,2-Gal*f* linkages; Man had terminal Man*p*, 1,2-Man*p*, 123-Man*p* and 126-Man*p* linkages; Glc had 1, 4-Glc*p* and terminal Glc*p* linkages. Among these linkages, the terminal Gal*f*, 1,2-Gal*f*, 1,2-Man*p*, 126-Man*p* and 1,4-Glc*p* linkages were the major residues in the Pc0−1. However, the absence of terminal-Gal*f*, 1, 2-Gal*f* and the linkages of Ara in the hydrolysate (P-2) indicated that these galactofuranosyl and arabinopyranosyl residues could easily hydrolyze on treatment with mild acid and, thus, could be located at the end of branches. Studies have found that hydrolysis of some galactofuranose units occur relatively quickly at a pH of 3.5. The furanosic glycosidic linkages which were sensitive to acid could get a certain degree of hydrolysis, even at room temperature with weak acid condition (Arata et al., 2016). Thus, if the galactofuranose were located at the backbone, the partial acid hydrolysis would cause the initial degradation of the polysaccharide to be complete oligosaccharides at the first step. No main chain structure could be left. The amount of 1,4-Glc*p* was decreased significantly in P-2, indicating Glc*p* was also in the side-chains but was more stable towards hydrolysis than Gal*f* or Ara*p*. In contrast, 1,2-Man*p* increased dramatically becoming the dominant sugar residue in the P-2 hydrolysate, accounting for 65 % of all the linkage patterns. 1,2-Man*p*, 126-Man*p* and 123-Man*p* were also present in P-2 with 20 % of the total linkages. Combining these data, we could obtain clear structural information for Pc0−1. Pc0−1 has a backbone of 1, 2-Man*p* and branches at 3-*O* and 6-*O* positions of 1,2-Man*p*. The side-chains are composed of 1,4-Glc*p*, terminal Gal*f*, 1,2-Gal*f* linkages, terminal Ara*p*, 1,4-Ara*p* and 134-Ara*p* linkages. The total ion current chromatogram and MS of partially *O*-methylated alditol acetates of Pc0−1 were shown in the supplementary material.

**Table 2**
GC–MS data analysis of partially *O*-methylated alditol acetates of Pc0-1 and the fractions after partial acid hydrolysis P-2.

| Methylation product | Linkage type | Main MS (*m/z*) | Molar ratio (%) | |
|---|---|---|---|---|
| | | | Pc0−1 | P-2 |
| 1,5-$Ac_2$-2,3,4-$Me_3$-L-Ara | Ara*p*(1→ | 101,117,129,145,161 | 3 | — |
| 1,4,5-$Ac_3$-2,3-$Me_2$-L-Ara | →4)Ara*p*(1→ | 101,117,129,161,189 | 8 | — |
| 1,3,4,5-$Ac_4$-2-Me-L-Ara | →3,4)Ara*p*(1→ | 117, 127,159,261 | 6.7 | — |
| 1,5-$Ac_2$-2,3,4,6-$Me_4$-D-Man | Man*p*-(→ | 101,117,129,145,161,205 | 15 | — |
| 1,5-$Ac_2$-2,3,4,6-$Me_4$-D-Glc | Glc*p*-(→ | 101,117,129,145,161,205 | 61 | — |
| 1,4-$Ac_2$-2,3,5,6-$Me_4$-D-Gal | Gal*f*(1→ | 101,117, 161,205,277 | 70 | — |
| 1,2,5-$Ac_3$-3,4,6-$Me_3$-D-Man | →2)Man*p*(1→ | 129,161,189 | 100 | 100 |
| 1,4,5-$Ac_3$-2,3,6-$Me_3$-D-Glc | →4)-Glc*p*-(→ | 101,113,117,131,161,173,233 | 92 | 12 |
| 1,2,4-$Ac_3$-3,5,6-$Me_3$-D-Gal | →2)Gal*f*(1→ | 101,117,129,143,161 | 62 | 5.2 |
| 1,5,6-$Ac_3$-2,3,4-$Me_3$-D-Man | →6)Man*p*(1→ | 101,117,129,161,189 | 5 | — |
| 1,2,3,5-$Ac_4$-4,6-$Me_2$-D-Man | →2,3)Man*p*(1→ | 101,129,161,261 | 25 | 11 |
| 1,2,5,6-$Ac_4$-3,4-$Me_2$-D-Man | →2,6)Man*p*(1→ | 129,189 | 45 | 17 |

1,2,5-Ac3−3,4,6-Me3-D-Man was used as the reference of the molar ratio.

### 3.4. NMR analysis

In the $^1$H NMR spectrum (Fig. 3a), eight anomeric signals in the region 5.2−4.95 ppm were designated as **A**–**H** based on the decreasing chemical shifts of their anomeric protons. At $\delta$ 5.1 ppm we observed two overlapped anomeric protons, which were determined from two cross resonance signals to correspond to $\delta$ 5.10/103.5 and $\delta$ 5.10/99.6 in HSQC spectrum (Fig. 3d). The $^{13}$C NMR spectrum (Fig. 3b) contained seven major signals ($\delta$ 107.6, 105.7, 103.5, 102.1, 100.5, 99.6 and 98.0) in the anomeric carbon region ($\delta$ 90–110). The signals at 105.7 and 107.6 ppm were attributed to anomeric carbons of β-galactofuranose units, which were due to their low-field resonances (Calixto et al., 2010; Gómez-Miranda et al., 2003).

Several residues were assigned and identified by 2D correlation experiments (COSY, TOCSY and HSQC). The carbon coupling of the anomeric protons was observed in the HSQC spectrum. The signals of **E** (5.03/105.7) and **G** (4.96/107.6) represent two different galactofuranose residues. Moreover, the H—H COSY experiment (Fig. 3c) demonstrated the coupling of the H1/H2 of unit **E** and **G** at 5.03/4.11 and 4.96/3.98, respectively. HSQC spectrum further showed that these H2/C2 at 4.11/86.9 (unit **E**) and 3.98/82.4 (unit **G**). The extreme downfield shifts of C2 at 86.4 ppm also confirmed that **E** had 2-*O* substitution. These observations revealed **E** was a (1→2)-β-D-Gal*f* and **G** was a terminal β-D-Gal*f* (Carbonero et al., 2005; Chen et al., 2016; Svensson et al., 2011; Zhou et al., 2019). For residues **A**, **D** and **H**, these three residues were assigned as different types of glucose units according to upfield chemical shifts of H2 ($\delta$ 3.66, 3.7 and 3.61). Compared with the reference (Wang et al., 2019), the downfield shift of C4 at $\delta$ 80.9 confirmed that residue **D** was →4)-α-D-Glc*p*-(1→ and residue **A** was terminal α-Glc*p*. For residue **H**, the downfield resonance of C4 at $\delta$ 80.9 and C6 at $\delta$ 65.9 indicated 4-*O* and 6-*O* substitutions. Proton signal at $\delta$ 3.13 had a corresponding carbon signal at $\delta$ 56.85, suggesting the presence of OMe. The inter-residual cross signals at $\delta$ 3.13/65.9 and $\delta$ 3.58/53.8 in HMBC spectrum (Fig. 3e) suggests that OMe group is linked to the C6 position of residue **H**. These evidences demonstrated that residue **H** was →4)-α-6-*O*-Me-α-Glcp-(1→. For residue **B,** the coupling of H1/C1 at 5.12/100.8 and H2/C2 at 4.1/81.9 confirmed it represented (1→2)-α-D-Man*p*. Signal **C** was related to the two other anomeric carbon signals in the HSQC. The coupling of H1/C1 at 5.1/103.5 was the signal of terminal α-D-Man*p*, while that of H1/C1 at 5.10/99.6 was the signal of (1→2,3)-α-D-Man*p,* which was determined by the downfield shift of the resonances C2($\delta$ 81.45) and C3 ($\delta$ 80.2). Residue **F** was confirmed to be (1→2,6)-α-D-Man*p* based on C2($\delta$ 78.2), C6 ($\delta$ 65.6) and the reference (Chen et al., 2011). Because of difficulty in the complete assignment of all the overlapped signals, the proton and carbon chemical shifts of some of the major residues are assigned in Table 3.

The HMBC was used to provide the correlations between the sugar residues and confirm linkage sequences among the major residues. The cross-peaks **A** H1/C4 **D** and $\mathbf{C_2}$ H3/C1 **D** revealed that terminal α-Glc*p* was linked to C4 of →4)-α-D-Glc*p*-(1→, and →4)-α-D-Glc*p*-(1→ was linked to C3 of (1→2,3)-α-D-Man*p*. The cross-peaks **E** H1/C6 **F** indicated

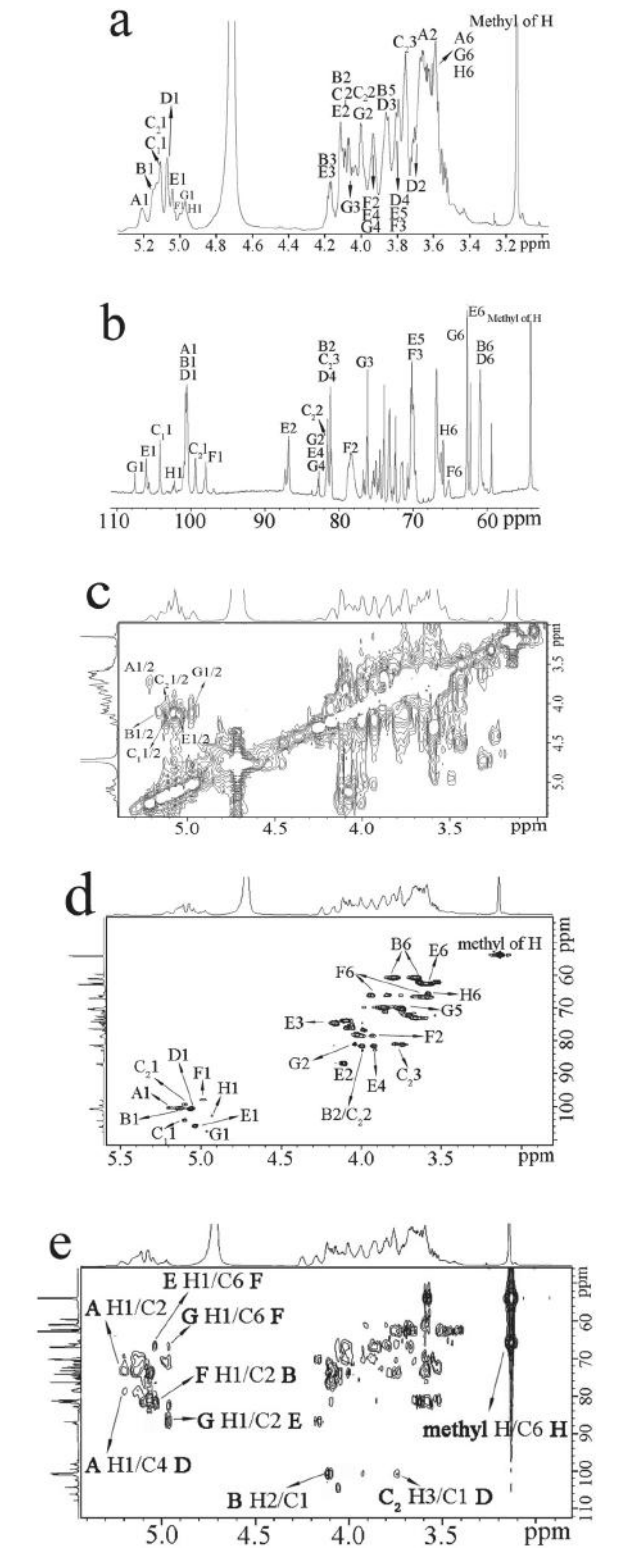


**Fig. 3.** NMR spectra of the polysaccharide Pc0-1. (**a**) $^{1}$H NMR spectrum; (**b**) $^{13}$C NMR spectrum; (**c**) $^{1}$H–$^{1}$H COSY spectrum in the anomeric region; (**d**) $^{1}$H–$^{13}$C HSQC spectrum; (**e**) $^{1}$H–$^{13}$C HMBC spectrum in the anomeric region.

**Table 3**
$^{1}$H and $^{13}$C NMR chemical shifts ($\delta$) for the residues of galactoglucomannan Pc0-1.

| Residue | H1/C1 | H2/C2 | H3/C3 | H4/C4 | H5/C5 | H6/C6 | Me |
|---|---|---|---|---|---|---|---|
| **A** | 5.2 | 3.61 | 3.74 | 3.40 | — | — | |
| α-Glc*p*(1→ | 100.46 | 73.2 | | 69.1 | — | — | |
| **B** | 5.14 | 4.1 | — | 3.75 | 3.85 | 3.66, 3.8 | |
| (1→2)-α-Man*p* | 100.6 | 81.9 | — | 66.6 | 71.35 | 60.8 | |
| **C$_1$** | 5.1 | 4.11 | — | — | — | — | |
| α-Man*p*(1→ | 103.5 | 73.9 | — | — | — | — | |
| **C$_2$** | 5.1 | 3.99 | 3.74 | 3.61 | — | — | |
| (1→2,3)-α-Man*p* | 99.6 | 81.45 | 80.2 | 72.9 | — | — | |
| **D** | 5.07 | 3.7 | 3.85 | 3.79 | 3.75 | 3.66,3.8 | |
| (1→4)-α-Glc*p* | 100.56 | 72.5 | 71.2 | 80.9 | 70.6 | 60.8 | |
| **E** | 5.03 | 4.11 | 4.16 | 3.92 | 3.80 | 3.62 | |
| (1→2)-β-Gal*f* | 105.7 | 86.9 | 74.6 | 82.8 | 71.2 | 62.3 | |
| **F** | 4.98 | 3.92 | 3.80 | 3.66 | 3.7 | 3.6, 3.94 | |
| (1→2,6)-α-Man*p* | 98.0 | 78.2 | 70 | 66.7 | 72.6 | 65.6 | |
| **G** | 4.96 | 3.98 | 4.04 | 3.92 | 3.74 | 3.64, 3.53 | |
| β-Gal*f*(1→ | 107.6 | 82.4 | 77.9 | 82.8 | 70.9 | 62.3 | |
| **H** | 4.95 | 3.66 | — | 3.79 | 3.83 | 3.58 | 3.13 |
| (1→4)-6-Me-α-Glc*p* | 102.1 | 72.8 | — | 80.9 | 71.3 | 65.9 | 53.8 |

(1→2)-β- D-Gal*f* was linked to C6 of (1→2,6)-α-D-Man*p*. **G** H1/C6 **F** and **G** H1/C2 **E** indicated terminal β-D-Gal*f* could be linked to both C6 of (1→2,6)-α-D-Man*p* and C2 of (1→2,6)-α-D-Man*p*. **B** H2/C1 and **F** H1/C2 **B** indicated the backbone of the polysaccharide mainly consists of (1→2)-α-D-Man*p* (Kobayashi et al., 1995).

Based on the monosaccharide composition analysis, partial acid hydrolysis, methylation results and NMR spectra, a structure for Pc0−1 can be proposed. It has a core structure with the backbone of →2)-α-Man*p*(1→. 40 % of the residues in the backbone branched at the *O*-6 and *O*-3. The side-chains were composed of →4)-α-Glc*p*(1→, which were located outside of the Man core and mostly linked to *O*-6 of the →2)-α-Man*p*(1→. Some of the →4)-α-Glc*p*(1→ residues had 6-*O* methyl modification. The site of Gal was at a more outer position. This has an →2)-β-Gal*f*(1→ linked to *O*-3 of the →2)-α-Man*p*(1→. The signals of Ara are not identified in the NMR spectrum. It was difficult to determine the conformation of the Ara residues. Ara residues, which have a terminal Ara*p*, 1,4-Ara*p* and 134-Ara*p* linkages are located at the ends of the side-chains. In addition, single terminal α-Man*p*(1→ and β-Gal*f*(1→ residues are present in the side-chains. Based on these analyses, a likely primary structure for Pc0−1 is proposed (Fig. 4).

Recently, several studies were reported on the polysaccharides from *Paecilomyces cicada*. The structures of polysaccharides from the same species are variable with different sources or fermentation conditions. For example, a galactomannan in the ascocarps of *Cordyceps cicadae* SHING from Hong Kong is composed of (1→2)-α-D-Man*p* and (1→6)-α-D-Man*p* residues in the core. Some of these residues are substituted at *O*-6 and *O*-2 with single terminal α-Man*p*(1→ and β-Gal*f*(1→ groups and contain short chains of (1→2)-β-Gal*f* units (Ukai et al., 1982). The structure of Pc0−1 seems similar with the structure of this polysaccharide. The main differences are the polysaccharide from the ascocarps of *Cordyceps cicadae* SHING has more (1→6)-α-D-Man*p* residues in the backbone but no Glc appeared in its side-chains. A heteropolysaccharide from cultured *P. cicadae* (Miquel) Samson was reported showing the backbone consisted of 1,4-linked α-D-Glc*p* and 1,4-linked 6-O-Me-α-D-Glc*p* residues, with occasionally interrupted by (1→6)-β-Gal*f* unit (Wang et al., 2019). The same characteristics between this polysaccharide and Pc0−1 are that both have 1,4-linked α-D-Glc*p*, 1, 4-linked 6-O-Me-α-D-Glc*p* and β-D-galactofuranose. But the distributions

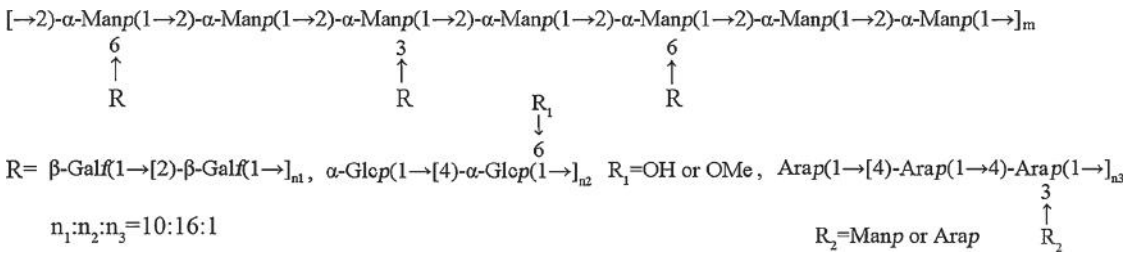


**Fig. 4.** The proposed main structure of the polysaccharide Pc0-1.

of Glc of the two polysaccharides are different. The polysaccharides from cultured *P. cicadae* have Glc in the main chain, while Pc0−1 has Glc in the side-chains. The linkages of β-D-galactofuranose are also different. In particular, the polysaccharide from cultured *Paecilomyces cicadae* has much less Man than Pc0−1. These structural analyses provide interesting information in chemotaxonomic studies and demonstrate the impact of growth conditions on the structures of these polysaccharides. The sources, molecular properties, chemical structures and bioactivities are summarized in Table 4.

Could *P. cicadae* be used as an alternative to *C. sinensis*? For polysaccharides in *C. sinensis*, the structures of polysaccharides have high diversity. Galactoglucomannan and galactomanan are the typical polysaccharides in *C. sinensis* and have comb-like structure. The core structures are composed of D-mannopyranosyl residues with the linkages of 1, 2-linked, 1, 23-linked and 1, 46-linked α-D-Man*p*. The side chains are mainly composed of 1, 5-linked, 1, 6-linked, 1, 2-linked β-Gal*f*. The glucose are located at the side chains with different linkages. Some differences in the linkage mode were observed. The structure varied according to the resources and growth conditions of *C. sinensis*. Overall, the structure of glucogalactomannan from *P. cicadae* was largely the same as that of *C. sinensis* (Mannan as the core structure, galactofuranose as the side chain). We therefore concluded that different polysaccharide from the genus Cordyceps have similar structure characteristics. We therefore concluded that different polysaccharide from the genus Cordyceps have similar structure characteristics, meaning that *P. cicadae* could be used as an alternative to *C. sinensis* to obtain polysaccharides (Nxumalo et al., 2020; Yan et al., 2014).

### 3.5. Determination of macrophage activation activity

Cell viabilities (Fig. 5a) were assessed by MTT assay on the cells treated with LPS and different concentrations of Pc0−1 for 24 h. The results showed that Pc0−1 was not cytotoxic to RAW264.7 cells. Compared with the control, Pc0−1 showed significant proliferation activity at the concentration range of 50–400 μg/mL.

The activation of macrophages could increase the production of reactive oxygen species (ROS), which is important in immune response related signaling pathways and plays a positive role in preventing and killing microbial invasion and in tumor genesis (Rendra et al., 2019). The production of ROS was measured using the fluorescent probe DCFH-DA. The fluorescence microscopy results showed the mean fluorescence intensity of DCF in LPS and Pc0−1 treated cells was significantly greater than that in the control (Fig. 5b), which demonstrated that the cells treated with Pc0−1 in the concentration range of 50–200 μg/mL displayed up-regulation of intracellular ROS production (Fig. 5c).

Macrophages play an important role in host defense systems. When the body is stimulated by pathological material or injury, macrophages can be activated from static state and destroy the targeted foreign organisms indirectly by enhancing the release of NO, iNOS, ROS, and several related cytokines (Murray & Wynn, 2011).

The impact of Pc0−1 on the pinocytic activity of RAW264.7 cells was examined using the neutral red uptake assay. The cells visibly increased after treatment with Pc0−1 compared to the normal control (Fig. 5d). The results indicate that macrophages treated with Pc0−1 exhibit strong pinocytic activity. Pc0−1 exhibited significant macrophage activation activity at the range of 50–400 μg/mL (Fig.5e).

The release of NO by macrophages regulates the inflammatory response and can activate functions of the immune system. When

**Table 4**
Polysaccharides originated from *Cordyceps cicadae* fungi: source, chemical structures and bioactivities.

| Fungus | polysaccharide resource | component | molecular weight | linkage | bioactivity | reference |
|---|---|---|---|---|---|---|
| Isaria cicadae Miquel | fruit body | Glc:Man:Gal = 1.70:1.37:1.00 Glc:Man:Gal = 5.41:1.04:1.00 | 30.9 kDa 555.3 kDa | – | Immunomodulatory activity | Xu et al., 2018 |
| ***Cordyceps cicadae* SHING** | Ascocarps | Man:Gal= 4:3 | 27 kDa | Backbone:(1→2)-α-D-Man*p* and (1→6)-α-D-Man*p*. Side chain: terminal β-Gal*f*, (1→2)-β-Gal*f* and terminal α-D-Man*p* occupied at O-6 and O-2 of the backbone | – | Ukai et al., 1982 |
| *Cordyceps cicadae* | Ascocarps | Glc:Man:Gal = 2.08:1.00:1.28 Glc:Man:Gal = 8.75:1.22:1.00 | – | – | Antioxidant activity | Olatunji et al., 2016 |
| *Paecilomyces cicadae* | Mycelium | Man:Rha: 3-O-Me-Gal: Glc: Gal=, 47.9:3.1:6.4:0.9:0.8. | 30.9 kDa | A backbone of 1,4-linked L-Rha and 1,6-linked D-Man*p* residues with branches at O-3 of D-Man*p* residues. Its side chain was comprised of minor terminal D-Glc and 1,4-linked 3-O-Me-D-Gal*p* residues terminated by D-Gal | – | (Wei et al., 2016) |
| *Paecilomyces cicadae* (Miquel.) Samson | Mycelium | Glc: Gal: Man = 23.8:2.1:1.0. | 22.3 kDa | Backbone consisted of 1,4-linked α-D-Glc*p* and 1,4-linked 6-O-Me-α-D-Glc*p* residues, which were occasionally interrupted by branched through 1,6-linked β-Gal*f* residues | Antioxidant activity | Wang et al., 2019 |

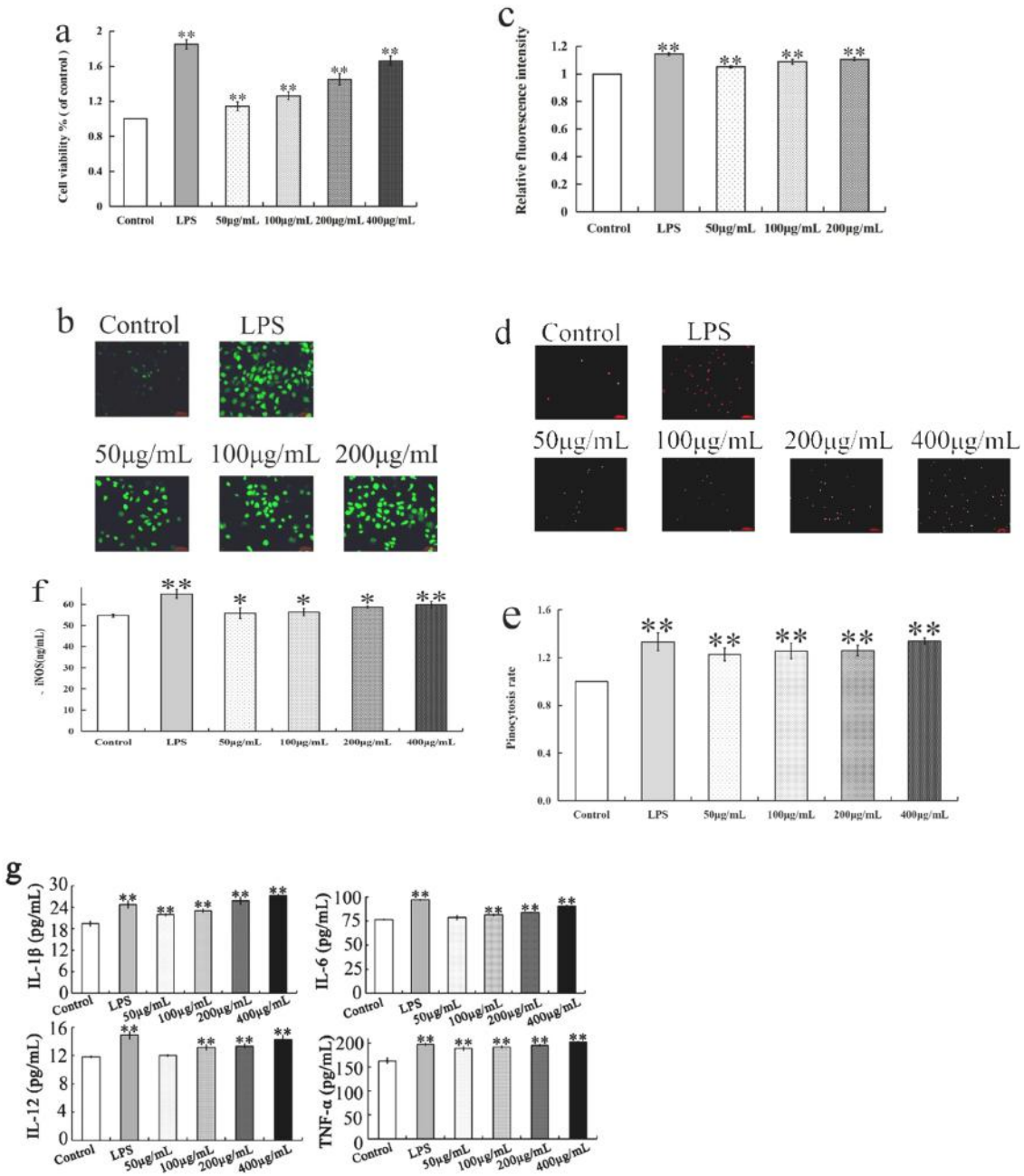


**Fig. 5.** Immunomodulatory activity of Pc0-1 in RAW264.7 macrophages. (**a**) Effects of Pc0-1 on cell proliferation. (**b**) Effect of Pc0-1 on ROS fluorescence. (**c**) ROS production. (**d**) RAW264.7 cells phagocytosed endocytic fluorescent-red latex beads (red fluorescence). (**e**) Phagocytic activity of RAW 264.7 cells stimulated by Pc0-1. (**f**) The effect of Pc0-1 on the levels of iNOS. (**g**) The effect of Pc0-1 on the levels of IL-1β, IL-6, IL-12 and TNF-α in RAW264.7. The results were expressed as means ± SD ($n = 3$). $^{*}P < 0.05$,$^{**}P < 0.01$ vs. control group.

macrophages are activated, they can express iNOS, the most important enzyme catalyzing NO production (Stewart, 2012). Effects on the iNOS secretion by macrophages were observed at Pc0−1 concentrations ranging 50−400 μg/mL, increased iNOS concentrations in a dose-dependent manner (Fig.5f).

IL-1β, IL-6, IL-12 and TNF-α are important cytokines produced to activate macrophages and regulate the immune response (Arango Duque & Descoteaux, 2014). Pc0−1 increased IL-1β and TNF-α production in a dose-dependent manner at 50–400 μg/mL, while it increased the production of IL-6 and IL-12 in the range of 100−400 μg/mL (Fig. 5g) ($P <$ 0.05).

Macrophages were used to investigate the immunoregulation activity of Pc0−1 due to their important role in the immune system. The results show that Pc0−1 not only improved the proliferation and phagocytosis of macrophages, but it also induced the secretion of NO, iNOS, ROS, and several related cytokines, such as IL-1β, IL-6, IL-12 and TNF-α ($P <$0.05).

### 3.6. Inhibition of cytokine production using anti-PRR antibodies

Based on literature, the innate immune system recognizes microorganisms through a limited number of germline-encoded pattern recognition receptors (PRRs), called the pathogen- associated molecular patterns (PAMPs). Related research showed different PRRs react with specific PAMPs, having distinct expression patterns, activating specific signaling pathways, and leading to distinct anti-pathogen responses (Zhu et al., 2018). The reported evidence suggest that polysaccharides from *P. cicadae* can activate macrophages to trigger an immunoregulatory response, but limited information is available on the cell membrane receptors involved in this immune-enhancing capacity to macrophages. Hence the antibodies response to TLR2, TLR4 and MR were used in the experiments to determine whether they play a role in Pc0−1 mediated immune enhancement in RAW 264.7 cells. The antibodies can bind to the receptors and prevent the polysaccharide from binding to the receptors and then depress the immunoregulatory (Kawai & Akira, 2011).

After pre-treatment of the cells with the three antibodies, the levels of iNOS and IL-6 secreted by the cells were significantly reduced, especially for the anti-MR group, which indicated Pc0−1 could act with all these three receptors and MR could be the major receptor of Pc0−1. The experiment also found that the pre-treatment of cells with anti-MR significantly reduced the levels of IL-12, IL-1β and TNF-α. Furthermore, anti-TLR2 can significantly change the level of TNF-α. After anti-TLR4 pretreatment, the level of IL-12 secretion is significantly reduced (Fig. 6). Therefore, we speculate that all these three receptors may participate in recognizing Pc0−1 and increase the secretion of iNOS and IL-6 by a series of immunomodulation. MR receptors could also be involved in immune regulation promoting the secretion of IL-12, IL-1β. In addition, we also found that TLR2 receptor is involved in the process of cell recognition of Pc0−1 and secretion of TNF-α, and TLR4 is involved in the process of IL-12 secretion.

Immunomodulation is the most notable biological function of fungi polysaccharides, which is associated with their role as biological response modifiers. An important feature of the bioactivity of immunomodulatory polysaccharides is the structure-function relationship. Several studies show that mannan especially branched mannan is an important agent for host fungal interactions through MR receptor. and induced the cytokine response (Yadav et al., 2020). Thus the core mannan could be a critical structure for the immunomodulatory activity of Pc0−1. Some studies have revealed that the Gal*f*-containing side chains have an impact on its immunomodulatory activity. *Trebouxia* sp., the algal symbiont of the lichen *Ramalina gracilis* demonstrated a galactofuranose-rich heteropolysaccharide, which was predominated by (1→5)-linked galactofuranosyl units in the side. This polysaccharide showed cell eliciting activity on peritoneal macrophages *in vitro*. Interestingly, the galactofuranosyl side chain displayed a potential role in the recognition process (Wang et al., 2020). Thus, further research could investigate the role of galactofuranose in immunomodulation of polysaccharides.

## 4. Conclusion

A heteropolysaccharide (Pc0−1) with molecular weight of $18 \times 10^3$ kDa was extracted from the spores of *P. cicadae*. The comprehensive structural analysis of Pc0−1 revealed that it consists of glucose, galactose, mannose and arabinose in the molar ratio of 8:5:4:1. Some of the glucose had methyl modification at *O*-6 position. It had a core structure consisted of 1, 2-linked α-D-Man*p* residues and branches at *O*-3 and *O*-6 of α-D-Man*p* residues. Its side-chains were comprised of 1, 4-linked α-D-Glc*p* and 1,4-linked 6-*O*-Me-α-D-Glc*p* residues. 1, 2-linked β-Gal*f* and minor 1, 4-linked Ara*p* and 134-linked Ara*p* residues were occasionally linked at the outside of the side- chains. The side-chains were terminated by single terminal α-D-Glc*p*, α-Man*p*, β-Gal*f* and Ara*p* (minor).

Pc0−1 exhibits moderate immunomodulatory activity by increasing the production of NO and enhancing the secretion of major inflammatory cytokines by macrophages, such as TNF-α, IL-1β, IL-6, in RAW 264.7 cells. To investigate the membrane receptor, we examined the effect of Pc0−1 on induced NO and cytokine productions in macrophages using anti-PRR antibodies, the results show that Pc0−1 mainly activates macrophages through the MR. TLR4 and TLR2 also participates in the recognition of Pc0−1.

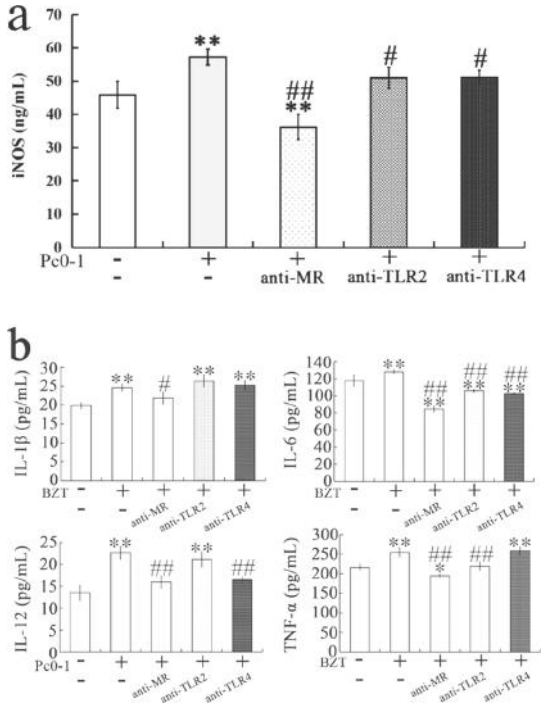


**Fig. 6.** Roles of MR, TLR2 and TLR4 on Pc0-1 induced immunomodulatory activity in RAW264.7 macrophages. (a) Roles of MR, TLR2 and TLR4 on Pc0-1 induced iNOS in RAW 264.7 cells. (b) Roles of MR, TLR2 and TLR4 on Pc0-1 induced the levels of cytokines in RAW264.7 cells. The results were expressed as means ± SD (n = 3). **P < 0.01, *P < 0.05,the group treated with antibodies compared to the negative control group ; ##P < 0.01, #P < 0.05, the group treated with antibodies compared to the group treated with only Pc0-1.

Overall, the polysaccharides from *P. cicadae* are largely the same as that of *C. sinensis* in structure and function and could be an important candidate for the bioactive polysaccharides of *C. sinensis*.

## Declaration of Competing Interest

The authors declare no conflicts of interest.

## Acknowledgments

This work was supported by National Natural Science Foundation of China (41406142); Natural Science Foundation of Zhejiang Province, China (LGF19D06004, LQ18D060005 and LGN18D060002)

## Appendix A. Supplementary data

Supplementary material related to this article can be found, in the online version, at doi:https://doi.org/10.1016/j.carbpol.2020.117462.

## References

Arango Duque, G., & Descoteaux, A. (2014). Macrophage cytokines: Involvement in immunity and infectious diseases. *Frontiers in Immunology, 5*, 491-491.

Arata, P. X., Quintana, I., Raffo, M. R., & Ciantia, M. (2016). Novel sulfated xylogalactoarabinans from green seaweed *Cladophora falklandica*: Chemical structure and action on the fibrin network. *Carbohydrate Polymers, 154*, 139–150.

Bao, X., Liu, C., Fang, J., & Li, X. (2001). Structural and immunological studies of a major polysaccharide from spores of Ganoderma lucidum (Fr.) karst. *Carbohydrate Research, 332*(1), 67–74.

Calixto, R., Mattos, B., Bittencourt, V., Lopes, L., Souza, L., Sassaki, G., Cipriani, T., Silva, M., & Barreto-Bergter, E. (2010). β-Galactofuranose-containing structures present in the cell wall of the saprophytic fungus Cladosporium (Hormoconis) resinae. *Research in Microbiology, 161*(8), 720–728.

Carbonero, E. R., Cordeiro, L. M. C., Mellinger, C. G., Sassaki, G. L., Stocker-Wörgötter, E. J., Gorin, P. A., & Iacomini, M. (2005). Galactomannans with novel structures from the lichen Roccella decipiens Darb. *Carbohydrate Research, 340*(10), 1699–1705.

Chen, Y., Mao, W. J., Yan, M. X., Liu, X., Wang, S. Y., Xia, Z., Xiao, B., Cao, S. J., Yang, B. Q., & Li, J. (2016). Purification, Chemical Characterization, and Bioactivity of an Extracellular Polysaccharide Produced by the Marine Sponge Endogenous Fungus Alternaria sp. SP-32. *Marine Biotechnology, 18*, 301–313.

Chen, Y., Mao, W. J., Tao, H. W., Zhu, W. M., Qi, X. H., Chen, Y. L., Li, H. Y., Zhao, C. Q., Yang, Y. P., Hou, Y. J., Wang, C. Y., & Li, N. (2011). Structural characterization and antioxidant properties of an exopolysaccharide produced by the mangrove endophytic fungus Aspergillus sp. Y16. *Bioresource Technology, 102*, 8179–8184.

Gómez-Miranda, B., Prieto, A., Leal, J. A., Ahrazem, O., Jiménez-Barbero, J., & Bernabé, M. (2003). Differences among the cell wall galactomannans from Aspergillus wentii and Chaetosartorya chrysella and that of Aspergillus fumigatus. *Glycoconjugate Journal, 20*(4), 239–246.

Huang, D., Meran, S., Nie, S. P., Midgley, A., Wang, J., Cui, S. W., Xie, M. Y., Phillips, G. O., & Phillips, A. O. (2018). Cordyceps sinensis: Anti-fibrotic and inflammatory effects of a cultured polysaccharide extract. *Bioactive Carbohydrates and Dietary Fibre, 14*, 2–8.

Ishurd, O., & Kennedy, J. (2005). The anti-cancer activity of polysaccharide prepared from Libyan dates (Phoenix dactylifera L.). *Carbohydrate Polymers, 59*, 531–535.

Kawai, T., & Akira, S. (2011). Toll-like receptors and their crosstalk with other innate receptors in infection and immunity. *Immunity, 34*(5), 637–650.

Kim, H. S., Kim, Y. J., Lee, H. K., Ryu, H. S., Kim, J. S., Yoon, M. J., Kang, J. S., Hong, J. T., Kim, Y., & Han, S. B. (2012). Activation of macrophages by polysaccharide isolated from Paecilomyces cicadae through toll-like receptor 4. *Food and Chemical Toxicology, 50*(9), 3190–3197.

Kobayashi, H., Watanabe, M., Komido, M., Matsuda, K., Ikeda-Hasebe, T., Suzuki, M., … Suzuki, S. (1995). Assignment of 1H and 13C NMR chemical shifts of a d-mannan composed of α-(1 → 2) and α-(1 → 6) linkages obtained from Candida kefyr IFO 0586 strain. *Carbohydrate Research, 267*(2), 299–306.

Murray, P. J., & Wynn, T. A. (2011). Protective and pathogenic functions of macrophage subsets. *Nature Reviews Immunology, 11*(11), 723–737.

Nie, S., Cui, S. W., & Xie, M. (2018). Chapter 4 - Cordyceps polysaccharides. In S. Nie, S. W. Cui, & M. Xie (Eds.), *Bioactive polysaccharides* (pp. 143–204). Academic Press.

Nxumalo, W., Elateeq, A. A., & Sun, Y. F. (2020). Can Cordyceps cicadae be used as an alternative to Cordyceps militaris and Cordyceps sinensis? – A review. *Journal of Ethnopharmacology, 257*, Article 112879.

Olatunji, O. J., Feng, Y., Olatunji, O. O., Tang, J., Wei, Y., Ouyang, Z., & Su, Z. (2016). Polysaccharides purified from Cordyceps cicadae protects PC12 cells against glutamate-induced oxidative damage. *Carbohydrate Polymers, 153*, 187–195.

Prasain, J. K. (2013). Pharmacological effects of cordyceps and its bioactive compounds. *Studies in Natural Products Chemistry, 40*, 453–468.

Qiu, P. P., Wu, F. X., Yi, L., Chen, L., Jin, S. Y., Ding, X. J., Ouyang, Y. L., Yao, Y. M., Jiang, Y., & Zhang, Z. Q. (2020). Structure characterization of a heavily fucosylated chondroitin sulfate from sea cucumber (*H. leucospilota*) with bottom-up strategies. *Carbohydrate Polymers, 240*, Article 116337.

Rendra, E., Riabov, V., Mossel, D. M., Sevastyanova, T., Harmsen, M. C., & Kzhyshkowska, J. (2019). Reactive oxygen species (ROS) in macrophage activation and function in diabetes. *Immunobiology, 224*(2), 242–253.

Sims, I. M., Carnochan, S. M., Bell, T. J., & Hinklay, S. F. R. (2018). Methylation analysis of polysaccharides: Technical advice. *Carbohydrate Polymers, 188*(15), 1–7.

Stewart, J. (2012). 9 - Innate and acquired immunity. In D. Greenwood, M. Barer, R. Slack, & W. Irving (Eds.), *Medical microbiology (eighteenth edition)* (pp. 109–135). Edinburgh: Churchill Livingstone.

Sun, X. F., Fowler, S. P., & Baird, M. S. (2005). Extraction and characterization of original lignin and hemicelluloses from wheat straw. *Journal of Agricultural and Food Chemistry, 53*(4), 860–870.

Svensson, M., Zhang, X., Huttunen, E., & Widmalm, G. (2011). Structural studies of the capsular polysaccharide produced by Leuconostoc mesenteroides ssp cremoris PIA2. *Biomacromolecules, 12*, 2496–2501.

Takano, F., Yahagi, N., Yahagi, R., Takada, S., Yamaguchi, M., Shoda, S., Murase, T., Fushiya, S., & Ohta, T. (2005). The liquid culture filtrates of Paecilomyces tenuipes (Peck) Samson (=Isaria japonica Yasuda) and Paecilomyces cicadae (Miquel) Samson (=Isaria sinclairii (Berk.) Llond) regulate Th1 and Th2 cytokine response in murine Peyer's patch cells in vitro and ex vivo. *International Immunopharmacology, 5*(5), 903–916.

Ukai, S., Matsuura, S., Hara, C., Kiho, T., & Hirose, K. (1982). Structure of a new galactomannan from the ascocarps of Cordyceps cicadae shing. *Carbohydrate Research, 101*(1), 109–116.

Wang, H., Zhao, J., Li, D., Song, S., Song, L., Fu, Y., & Zhang, L. (2015). Structural investigation of a uronic acid-containing polysaccharide from abalone by graded acid hydrolysis followed by PMP-HPLC–MSn and NMR analysis. *Carbohydrate Research, 402*, 95–101.

Wang, J. Q., Nie, S. P., Chen, S. P., Phillips, A. O., Phillips, G. O., Li, Y., Xie, M. Y., & Cui, S. W. (2018). Structural characterization of an α-1, 6-linked galactomannan from natural Cordyceps sinensis. *Food Hydrocolloids, 78*, 77–91.

Wang, T., Dong, Z., Zhou, D. J., Sun, K. L., Zhao, Y. Q., Wang, B., & Chen, Y. (2020). Structure and immunostimulating activity of a galactofuranose-rich polysaccharide from the bamboo parasite medicinal fungus *Shiraia bambusicola*. *Journal of Ethnopharmacology, 257*, Article 112833.

Wang, Y. B., He, P. F., He, L., Huang, Q. R., Cheng, J. W., Li, W. Q., Liu, Y., & Wei, C. (2019). Structural elucidation, antioxidant and immunomodulatory activities of a novel heteropolysaccharide from cultured Paecilomyces cicadae (Miquel.) Samson. *Carbohydrate Polymers, 216*, 270–281.

Wang, Y. T., Liu, Y. F., Yu, H. Z., Zhou, S., Zhang, Z., Wu, D., Yan, M. Q., Tang, Q. J., & Zhang, J. (2017). Structural characterization and immuno-enhancing activity of a highly branched water-soluble β-glucan from the spores of Ganoderma lucidum. *Carbohydrate Polymers, 167*, 337–344.

Wu, F., Zhou, C., Zhou, D., Ou, S., & Huang, H. (2017). Structural characterization of a novel polysaccharide fraction from Hericium erinaceus and its signaling pathways involved in macrophage immunomodulatory activity. *Journal of Functional Foods, 37*, 574–585.

Wu, F., Zhou, C., Zhou, D., Ou, S., Liu, Z., & Huang, H. (2018). Immune-enhancing activities of chondroitin sulfate in murine macrophage RAW 264.7 cells. *Carbohydrate Polymers, 198*, 611–619.

Xu, X., Yan, H., & Zhang, X. (2012). Structure and immuno-stimulating activities of a new heteropolysaccharide from Lentinula edodes. *Journal of Agricultural and Food Chemistry, 60*(46), 11560–11566.

Xu, Z. C., Yan, X. T., Song, Z. Y., Li, W., Zhao, W. B., Ma, H. H., Du, J. L., Li, S. J., & Zhang, D. (2018). Two heteropolysaccharides from Isaria cicadae Miquel differ in composition and potentially immunomodulatory activity. *International Journal of Biological Macromolecules, 117*, 610–616.

Yadav, B., Mora-Montes, H. M., Wagener, J., Cunningham, I., West, L., Haynes, K., … Gow, N. A. R. (2020). Differences in fungal immune recognition by monocytes and macrophages: *N*-mannan can be a shield or activator of immune recognition. *The Cell Surface, 6*, 100042.

Yan, J. K., Wang, W. Q., & Wu, J. Y. (2014). Recent advances in Cordyceps sinensis polysaccharides: Mycelial fermentation, isolation, structure, and bioactivities: A review. *Journal of Functional Foods, 6*, 33–47.

Yang, Y., Zhang, J., Liu, Y., Tang, Q., Zhao, Z., & Xia, W. (2007). Structural elucidation of a 3-O-methyl-d-galactose-containing neutral polysaccharide from the fruiting bodies of Phellinus igniarius. *Carbohydrate Research, 342*(8), 1063–1070.

Zhang, A., Sun, P., Zhang, J., Tang, C., Fan, J., Shi, X., & Pan, Y. (2007). Structural investigation of a novel fucoglucogalactan isolated from the fruiting bodies of the fungus Hericium erinaceus. *Food Chemistry, 104*(2), 451–456.

Zhou, D. J., Li, P. P., Dong, Z., Wang, T., Sun, K. L., Zhao, Y. Q., Wang, B., & Chen, Y. (2019). Structure and immunoregulatory activity of β-d-galactofuranose-containing polysaccharides from the medicinal fungus Shiraia bambusicola. *International Journal of Biological Macromolecules, 129*, 530–537.

Zhu, G., Xu, Y., Cen, X., Nandakumar, K. S., Liu, S., & Cheng, K. (2018). Targeting pattern-recognition receptors to discover new small molecule immune modulators. *European Journal of Medicinal Chemistry, 144*, 82–92.

Wei, C. Y., Li, W. Q., Shao, S. S., He, L., Cheng, J. W., Han, S. F., & Liu, Y. (2016). Structure and chain conformation of a neutral intracellular heteropolysaccharide from mycelium of Paecilomyces cicadae. *Carbohydrate Polymers, 136*, 728–737.